Arabian Journal of Chemistry (2016) xxx, xxx–xxx

King Saud University

Arabian Journal of Chemistry

www.ksu.edu.sa
www.sciencedirect.com

ORIGINAL ARTICLE

# The structure design of biotransformed unsymmetrical nitro-contained 1,5-diaryl-3-oxo-1, 4-pentadienyls for the anti-parasitic activities

**Zia Ud Din [a,*], Danielle Lazarin-Bidóia [b], Vanessa Kaplum [b], Francielle Pelegrin Garcia [b], Celso Vataru Nakamura [b], Edson Rodrigues-Filho [a,*]**

[a] *LaBioMMi, Departamento de Química, Universidade Federal de São Carlos, CP 676, 13.565-905 São Carlos, SP, Brazil*
[b] *Laboratório de Inovação Tecnológica no Desenvolvimento de Fármacos e Cosméticos, Universidade Estadual de Maringá, Av. Colombo 5790, 87020-900, Bloco B-08, Maringá, PR, Brazil*

Received 22 December 2015; accepted 24 March 2016

**KEYWORDS**

1,5-Diaryl-3-oxo-1, 4-pentadienyls; Dibenzalacetone; *Trypanosoma cruzi*; *Leishmania amazonensis*; *Penicillium brasilianum*

**Abstract** Two 1,5-diaryl-3-oxo-1,4-pentadienyls (**1** and **2**) having nitro group attached exhibited potent anti-parasitic activity when evaluated against *Trypanosoma cruzi* and *Leishmania amazonensis*. In the present work, metabolomic analysis revealed that enzymatic action of *T. cruzi* reduces the C=C bonds and let the nitro groups intact. Further, these two reduced compounds along with six other congeners were produced by chemical or microbiological methods and evaluated against *T. cruzi*. All reduced compounds showed less potency than compounds **1** and **2**, proving the importance of unsaturated moieties for activity. This investigation provides insight into the mechanism of action of nitro unsaturated diarylpentadienones reinforcing previous studies showing their interference in the redox metabolism of *T. cruzi*. In the result increase in reactive oxygen and nitrogen species occurs, altering mitochondrial function and depleting the whole antioxidant system, which ultimately causes parasite death. Docking studies using trypanothione oxy-reductase as target helped understanding the activities. The present investigation confirms that enzymes play a pivotal role in drug activation.


## 1. Introduction

According to the World Health Organization (WHO) report, the parasitic infections such as chagas disease and leishmaniasis still show worrying enhancements, especially in the developing countries (N°340, 2014). The lack of safe medication and the serious side effect caused by the use of available chemotherapy (McGreevy and Marsden, 1986), require intensive attention of the scientific community, in attempts to develop novel drugs for the treatment of these diseases.

* Corresponding authors. Tel.: +55 (016) 3351 8053; fax: +55 (016) 3351 8350.
E-mail address: zia.ufscar@gmail.com (Z.U. Din).
Peer review under responsibility of King Saud University.

Production and hosting by Elsevier

http://dx.doi.org/10.1016/j.arabjc.2016.03.005
1878-5352 © 2016 The Authors. Production and hosting by Elsevier B.V. on behalf of King Saud University.
This is an open access article under the CC BY-NC-ND license (http://creativecommons.org/licenses/by-nc-nd/4.0/).

Please cite this article in press as: Din, Z.U. et al., The structure design of biotransformed unsymmetrical nitro-contained 1,5-diaryl-3-oxo-1, 4-pentadienyls for the anti-parasitic activities. Arabian Journal of Chemistry (2016), http://dx.doi.org/10.1016/j.arabjc.2016.03.005

Recently, chalcones and related compounds emerged as a new class of anti-trypanosomatids agents (Roussaki et al., 2013). Other classes of compounds having nitro group have recently been revived for the advancement into clinical trials (Marin-Neto et al., 2009; Patterson and Wyllie, 2014; Priotto et al., 2009; Torreele et al., 2010), and many of them are in the market serving to cure anti-parasitic diseases (Patterson and Wyllie, 2014). It seems that nitro group in conjugation with other structural elements significantly increases anti-parasitic activity and yields more potent compounds (Boechat et al., 2015).

In our previous work (Zia et al., 2014), a series formed of 20 compounds inspired from the natural products chalcone and curcuminoid was synthesized and tested against *Trypanosoma cruzi* and *Leishmania amazonensis*. Among these substances, 2-methyl-1-(4-nitrophenyl)-5-p henylpenta-1,4-dien-3-one (**1**) and 2-methyl-1,5-bis(4-nitrophenyl)pen ta-1,4-dien-3-one (**2**) showed impressive results, with $IC_{50}$ lower than the commercial drug benznidazole. During following studies, it was observed that compounds **1** and **2** induce oxidative stress in three different forms of *T. cruzi*, causing damage in essential cell structures, reflecting in lipid peroxidation and DNA fragmentation (Bidóia et al., 2015).

Other researchers found that the anti-mycobacterial agent PA-824, which contains nitro group, is reduced by a deazaflavin (F420)-dependent nitroreductase (Ddn) in *Mycobacterium tuberculosis* (Singh et al., 2009) to amines. Nitroreductase (NTR) was also identified in trypanosomatid protozoa which are responsible for the activation of trypanocidal nitro compounds including Bzn, Nfx and also fexinidazole by reductive potential of NTR1 (Hall et al., 2011; Wilkinson et al., 2008). During similar studies, Romão et al. have shown that the antioxidant system, trypanothione/trypanothione reductase, is involved in protecting *Leishmania* against the toxic effect of nitrogen-derived reactive species (Romão et al., 2006).

In the present study, efforts were made in order to gain understanding in the metabolism and the structural requirements that affect activities of compounds derived from **1** and **2**, as these compounds have nitro group and electrophilic centers that may interact with co-enzymes glutathione and trypanothione, which are part of the redox system in these parasites. Thus we studied the metabolism of compounds **1** and **2** by *T. cruzi*. Further, compounds **1** and **2** were reduced by different chemo selective agent and were feed to *T. cruzi* to see either the compounds are active or not. *In silico* investigation revealed target systems for compounds **1** and **2**.

## 2. Results and discussion

### 2.1. Chemistry

#### 2.1.1. Transformation of compounds *1* and *2* by *T. cruzi*

Compounds **1** and **2** were synthesized by classical acid catalyzed aldol reaction of nitrobenzaldehyde with unsymmetrical ketone (2-butanone) to yield an intermediate that was then treated with benzaldehyde or nitrobenzaldehyde in the presence of base to give **1** and **2**. These two nitro groups containing substances were very active when tested against different forms of *T. cruzi* and *L. amazonensis* (Bidóia et al., 2015; Zia et al., 2014).

Metabolomic profile of these compounds by *T. cruzi* was studied. Epimastigote form was exposed to 20 μM of **1** and **2** over six hours and then metabolites were extracted. After this treatment, approximately 90% of the parasites were found died. Parasites that were not exposed to compounds **1** and **2** were used as control for mass spectrometric analysis of both samples in parallel with reference compounds.

Cultivation medium containing *T. cruzi* with and without test substances was lyophilized prior to extraction. Extractions were performed by partitioning with ethyl acetate after suspending lyophilized powder in water successively at pH 7, 3 and 8, in order to cover the possibility of forming acid or basic compounds. Biotransformation products were detected only in the neutral extract.

Compounds **1** and **2** were consumed completely and produced metabolites 5 and 6, respectively. Compounds **1** ($C_{18}H_{15}NO_3$, 293 Da) and **2** ($C_{18}H_{14}N_2O_5$, 338 Da) exhibited $[M-H]^-$ peaks at *m/z* 292 and 337 in their respective APCI$^-$ mass spectrum, and showed a cinnamoyl UV absorption band with $\lambda_{max}$ at 318 and 323 nm, respectively. In both metabolites detected, the cinnamoyl absorption was substituted by a $\lambda_{max}$ at 277 (metabolite **5**, from **1**) and 279 (metabolite **6**, from **2**), and the molecular masses increased by 4 Da (*m/z* 296 and 341 for **5** and **6** respectively). These data in conjunction clearly indicated reduction of the two C—C double bond (Fig. 1). Metabolites **5** and **6** were also characterized by HRESI-MS, showing $[M+H]^+$ at 298.1443 ($C_{18}H_{20}NO_3$, cal. 298.1443) and 343.1301 ($C_{18}H_{19}N_2O_5$, cal. 343.1294) respectively.

#### 2.1.2. Synthesis of compounds *3–10*

Based on the above shown reductive biotransformation of the active compounds by *T. cruzi*, a series of substances derived from **1** and **2** was produced, all of them containing hydrogenated positions compared with precursors. These reduced compounds were all tested for *T. cruzi* inhibition. Compounds **3–10** (Fig. 2) were obtained by chemical or microbiological methods. Hantzsch ester hydrogenation (HEH) (Martin and List, 2006) produced compounds **3** and **4**, with reduction only at the less substituted C—C double-bound, while the whole cells of the fungus *Penicillium brasilianum* reduced both double-bounds resulting **5** and **6**. Sodium borohydride was used for carbonyl reduction (Warda and Rheea, 1989) of **1**

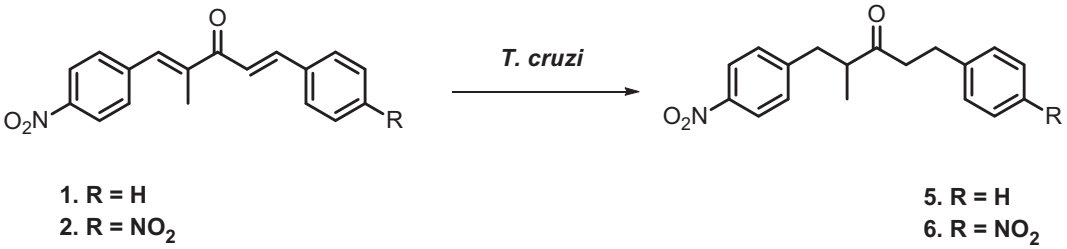


**Figure 1** Unsymmetrical 1,5-diaryl-3-oxo-1,4-pentadienyls **1** and **2** derived metabolites. The action of parasite reduced both double bonds.

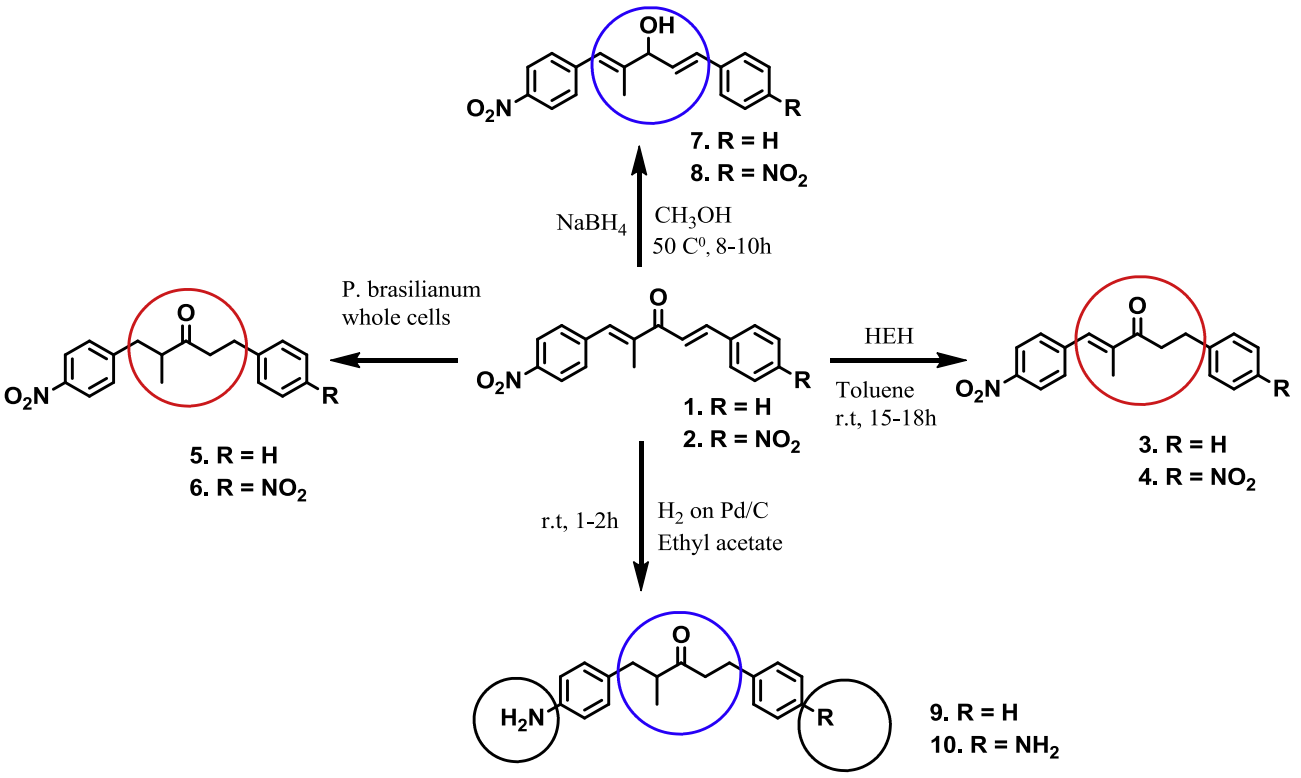


**Figure 2** Selective reduction of different groups by selective reagent and catalyst.

and **2** producing the alcohols **7** and **8**. When **1** and **2** were treated with $H_2$ on Pd/C (Aponte et al., 2008) the double bonds and nitro groups were reduced forming compounds **9** and **10**.

The synthesis and characterization of compounds **1** and **2** are reported elsewhere (Zia et al., 2014). The $^1$H NMR spectra of compounds **1** and **2** show the presence of a pair of doublets at $\delta_H$ 7.53 and 7.69, with a coupling constant of c.a. 16 Hz, typical for a *trans* two vinylic spins system. The $^{13}$C NMR of both compounds shows the characteristics C═O signal at c.a. $\delta_C$ 190. Compounds **3–10** show differentiation of some of NMR signals due to reduction of unsaturated moieties by specific reagents. The $^1$H NMR spectra of compounds **3** and **4** show the appearance of methylene protons at nearly $\delta_H$ 3.0, while disappearing CH═CH signal at $\delta_H$ 7.53 confirms the reduction of one CH═CH selectively. The $^1$H NMR spectra of **5** and **6** show the disappearance of two double bonds representative signal between $\delta_H$ 7 and 8, while the appearance of new methylenic signals between 2–3 ppm confirms the reduction of both double bonds in compounds **1** and **2**. The $^{13}$C NMR spectra show the disappearing of two signals between $\delta_C$ 120 and 140 and the appearance of two new signals between 30 and 40 ppm confirms the reduction of CH═CH. The $^1$H NMR spectra of compounds **7** and **8** show the appearance of doublet nearly $\delta_H$ 4.80, proving the reduction of carbonyl group. The $^{13}$C NMR confirms the reduction of carbonyl by disappearing the carbonyl signal at $\delta_C$ 190 and appearing of carbinolic signal for C—OH at $\delta_C$ 77.0. The $^1$H NMR of compounds **9** and **10** shows the disappearance of all CH═CH signals at $\delta_H$ 7.53 and 7.69, while appearing signal between 3 and 4 ppm confirms the reduction of olefin system. The detection of four signals in $^{13}$C NMR appeared due to methylenic carbons. The up-field shift in $^1$H NMR was observed in aromatic signals, which was due to the reduction of nitro to amino group. The Pd/C on hydrogen reduces double bonds along with nitro groups. The structures of all compounds were further established using UV–Vis and mass spectrometric analysis.

### 2.2. Metabolism and bioactivity study

Compounds **1** and **2** showed great anti-parasitic activities against *T. cruzi* and *L. amazonensis* (Table 1). They inhibited epimastigote form of *T. cruzi* exhibiting an $IC_{50}$ value (inhibitory concentration for 50% of the parasites) in micro molar concentration (Zia et al., 2014). Recently, we studied how these drugs act in *T. cruzi* and found that they cause an intense oxidative stress resulting in cell death by necrosis, autophagy and apoptosis. It was also observed that DNA fragmentation, intensification of lipid per oxidation, and reduction of free thiols levels occurred (Bidóia et al., 2015). In the present work we found that *T. cruzi* reduces the double-bonds of the dienone system present in **1** and **2**. This finding can be close related to the diminishing amount of free thiols groups in the parasite cells. Thiols groups are part of important cysteine containing co-enzymes in many organisms. Trypanothione (N1,N8-bis(glutathionyl)spermidine or $T(SH)_2$) is generated from glutathione by trypanothione synthetase and is the major redox mediator in *T. cruzi*. The enzyme containing $T(SH)_2$ can react with Michael acceptors such as enones and other α,β-unsaturated carbonyl groups containing substances. The scheme shown in Fig. 3 below could explain the observed physiological effects that **1** and **2** cause in *T. cruzi*, as well as the reduction of their C—C double bonds. Carbons C-1 in **1**,

**Table 1** Anti-parasitic and cytotoxic activity of compounds **1**–**10**.

| S. no | *T. cruzi* epimastigote | SI in epimastigotes | *L. amazonensis* promastigotes | SI in promastigotes | *VERO* cells |
|---|---|---|---|---|---|
| | $IC_{50}$ (μM) | | $IC_{50}$ (μM) | | $CC_{50}$ (μM) |
| 1 | 3.5 ± 0.4 | 13.5 | 13.4 ± 2.0 | 3.5 | 47.3 ± 4.2 |
| 2 | 1.8 ± 0.2 | 23.9 | 3.4 ± 0.1 | 10.1 | 43.0 ± 4.24 |
| 3 | 52.2 ± 1.6 | 4.8 | 6.8 ± 0.0 | 36.5 | 248.1 ± 15.3 |
| 4 | 11.9 ± 0.6 | 12.8 | 24.4 ± 2.4 | 6.3 | 152.7 ± 3.9 |
| 5 | 58.1 ± 0.9 | 2.4 | 20.2 ± 2.2 | 7.0 | 140.4 ± 5.23 |
| 6 | 15.3 ± 2.1 | 7.2 | 16.6 ± 1.8 | 6.7 | 110.9 ± 4.3 |
| 7 | >100 | – | 74.0 ± 4.0 | 4.4 | 323.8 ± 13.3 |
| 8 | 22.4 ± 1.62 | 13.5 | 23.7 ± 2.4 | 12.7 | 302.1 ± 15.8 |
| 9 | 89.8 ± 6.94 | 3.2 | 21.0 ± 1.8 | 13.8 | 260.3 ± 1.3 |
| 10 | 42.7 ± 4.45 | 10.0 | 21.0 ± 3.7 | 20.3 | 426.3 ± 8.2 |
| PC1 | 6.5 ± 0.7 | 94.6 | | | 614.7 ± 115.2 |
| PC2 | | | 0.06 ± 0.00 | | |

SI: Selectivity index; PC1 (positive control 1): Benznidazole; PC2 (positive control 2): Amphotericin B.

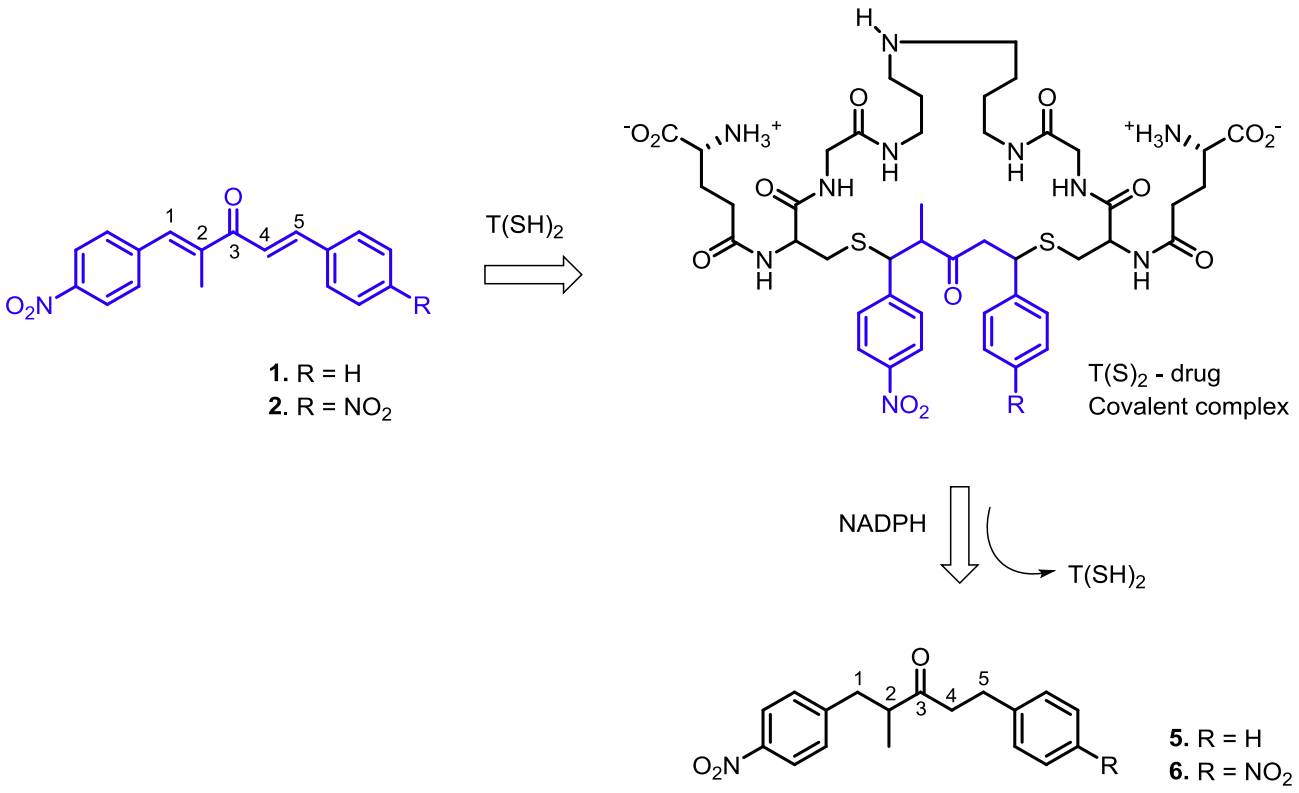


**Figure 3** Drug covalent interaction of **1** and **2** with trypanothione and reduction by NADPH.

and C-1 and C-5 in **2** are strongly electrophylic because they are β-enone and due the presence of the electron withdrawing $NO_2$ group at *para* position in the aromatic ring. Thus, **1** and **2** can be attacked by the thiols from coenzyme $T(SH)_2$, producing a $T(S)_2$ – drug covalent complex. This explains the diminishing of free SH groups in *T. cruzi* cells after exposed to **1** and **2**. The efforts of the cell machinery to regenerate the redox mediator $T(SH)_2$ may result in disruption of a portion of the covalent complex, producing an amount of reduced compounds **5** and **6**. Usually the reducing agent is NADPH.

In order to check the structural requirements for the activity of these diarylpentadienones some derivatives reduced at different positions were prepared by chemical and microbiological methods. Among compounds **3**–**10** (Fig. 2), **5** and **6** were obtained by bio-catalytic method using whole cells of *P. brasilianum* as biocatalyst (Murakami et al., 2013; Yamaguchi et al., 2011), because all synthetic catalyzing agents used failed to selectively reduce both double bonds. In *P. brasilianum* the enzyme OYE (old yellow enzyme) plays an important role in the reduction of double bonds.

Please cite this article in press as: Din, Z.U. et al., The structure design of biotransformed unsymmetrical nitro-contained 1,5-diaryl-3-oxo-1, 4-pentadienyls for the anti-parasitic activities. Arabian Journal of Chemistry (2016), http://dx.doi.org/10.1016/j.arabjc.2016.03.005

*T. cruzi* and *L. amazonensis* were treated with **3–10**, which are different reduced form of potent compounds **1** and **2**. In general the $IC_{50}$ values enhanced significantly for both parasites in comparison with values observed for parent compounds (Table 1). It means that double bonds are crucial for activity. In general it was seen that potency decreases by reducing any of the moiety of compounds **1** and **2**. Compounds having one bond reduced (**3** and **4**) face reduction in the potency and exhibit $IC_{50}$ 52.2 ± 1.6 and 11.9 ± 0.6 μM against epimastigote. By reduction of the two double bonds we get the compounds obtained by the metabolomic study, compounds **5** and **6**. These compounds also loss their potency and its $IC_{50}$ decreases to 58.1 ± 0.9 and 15.3 ± 2.1 μM against epimastigote. Compounds **7** and **8** undergone reduction of carbonyl and $IC_{50}$ reach to >100 and 22.4 ± 1.62 respectively. Compounds **9** and **10** that were obtained by the reduction of double bonds and $NO_2$ exhibit a complete loss of potency by showing $IC_{50}$ 89.8 ± 6.94 and 42.7 ± 4.45 μM respectively. These results are contrary to those published by others researchers, who found that nitroreductase enzymes present in *T. cruzi* (Wilkinson et al., 2008) and in *Leishmania danovani* (Wyllie et al., 2013), but not in the mammal cells, activate $NO_2$-containing drugs into a more active form. In those organisms, the trypanocidal activity of nitro compounds depends on nitroreductase enzymes **(**NTR**)** that converts them to amines, enhancing their activity (Hall et al., 2012).

In all the reduced products **3–10** it was observed that compounds derived from **2** maintain their activity up to little extent as compared to that derived from compound **1**. By losing potency the cytotoxicity against normal cell lines improved and it is also not harmful for it in high concentration. Greater the selectivity index (SI) value, better the drug candidate. Benznidazole has good SI (94.6) but is still inadequate due to pathogen resistance (Campos et al., 2014; Mejia et al., 2012) and its unsatisfactory treatment in the chronic phase of the disease (Garcia et al., 2005).

The SI value of compound **2** is better than compound **1**, being better candidate than **1**. All other reduced products **3–10** show poor selective index as related to their biological activity. In similar pattern the activity of compounds **3–10** also shows reduction for *L. amazonensis* (promastigotes), except for compound **3**, derived from **1**, which shows $IC_{50}$ value c.a. half of the parent compound, but with selectivity ten times better (Table 1).

### 2.3. Molecular docking

#### 2.3.1. Optimization of ligands

The structure of all compounds **1–10** was analyzed for their stability and optimized energy using software Avogadro which is an advanced semantic chemical editor, visualization, and analysis platform (Hanwell et al., 2012). Theoretical calculations were carried for best stable structure of compounds. Lower energy conformers were selected for docking calculation. It was observed that the planarity of compounds changed completely by reducing one or more bonds (Fig. 4). Thus, in case of compounds **3–10**, the aromatic rings go out of the plane, and the molecules gain conformational flexibility. For activity the planarity stability is crucial, and loss of activity occurred once the reduction of any moiety occurs.

#### 2.3.2. In silico interaction studies

All compounds were analyzed for their binding possibility to enzyme trypanothione *Pdb* code 1BZL and the result obtained are tabulated in Table 2. Active site calculation was performed

**Table 2** Docking results of compounds **1–10** docked on to trypanothione reductase (1BZL).

| Compounds | Binding energy (kcal $mol^{-1}$) | Inhibition constant (Temp = 298.15 k) ki μM | Calculated RMS from reference (Å) |
|---|---|---|---|
| 1 | −8.51 | 0.58 | 32.72 |
| 2 | −10.26 | 0.03 | 32.46 |
| 3 | −8.36 | 0.75 | 33.70 |
| 4 | −8.96 | 0.27 | 26.46 |
| 5 | −7.04 | 6.90 | 35.85 |
| 6 | −7.86 | 1.72 | 32.75 |
| 7 | −7.50 | 3.19 | 27.47 |
| 8 | −8.74 | 3.92 | 29.44 |
| 9 | −4.54 | 473 | 26.59 |
| 10 | −4.64 | 396 | 28.00 |

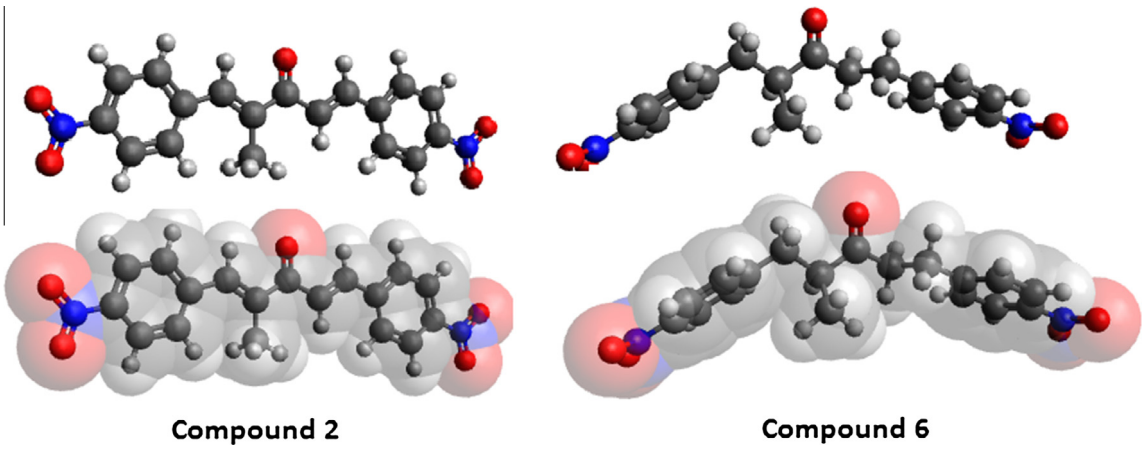


**Figure 4** Planarity loses as the result of reduction of double bonds in compound **2**, calculated by Avogadro 1.1.1.

on the basis of crystallized ligand in its crystal structure. Centroid of the active site was calculated and then all compounds were evaluated for their *in silico* inhibition study. The amino acids that contribute actively are Gly-12, Gly-14, Ser-15, Gly-16, Asp-36, Val-37, Ser-47, Ala-48, Gly-51, Thr-52, Cys-53, Val-56, Cys-58, Lys-61, Gly-126, Gly-128, Ala-160, Ser-161, Gly-162, Arg-288, Arg-291, Gly-326, Asp-327, Met-333, Leu-334, Thr-335, Pro-336, and Ala-338. Compounds **1–10** have interaction with amino acid in the active sites of 1BZL, and depend on the structure and pharmacophoric sites (Figs. 5a and 5b). Compound **1**, which is second potent compound, has interaction with amino acids Lys-61 by forming H-bond between Oxygen of nitro having bonded distance 2.5 Å. H-bond *pi* interaction between aromatic ring and Gly-16 by distance of 1.65 Å was also observed (Fig. 5a). Compound **2**, which is the most potent in the series, shows a good interaction with amino acids of the active site of enzyme. Several bonding interactions were calculated including H bond between Carbonyl and that of Thr-335 by distance 2.93 Å, H-bond between Gly-128 with oxygen of nitro group by distance of 3.16 Å, 2H bonds between Thr-335 with oxygen of nitro group by distance of 2.49 and 3.06 Å respectively. Also 1H bond between Gly-51 with oxygen of carbonyl by bonding distance of 3.40 Å along with 1 sigma pi interaction between Thr-52 and aromatic ring of ligand by distance of 3.4 Å were calculated (Fig. 5a).

Compound **2** and their derivatives have two nitro groups show greater interaction than compound **1** derivatives having one nitro group. Extra nitro group significantly increases all types of interaction including van der Waals, hydrogen bonding, water interaction, electrostatic and covalent bond interaction (Fig. 5a).

Compounds exhibited potency *in silico* were also active in wet laboratory experiment such as compounds **1**, **2**, **3**, **4**, **6** and **8**. The docking result is in agreement with in vitro assay results except compounds **4** and **8**, which show great inhibition *in silico* than wet laboratory experiment. Compound **4** having one bond and compound **8** having carbonyl reduced may probably give space to enzyme to be interacting more strongly. After reduction of these moieties it still maintains some degree of planarity, but when both double bonds are reduced the planarity loses completely. So the interaction forces become weak. These results showed that there is maximum probability that these compounds inhibit trypanothione reductase (see Fig. 6).

### *2.3.3. Studies on molecular orbitals by computational analysis*

The highest occupied molecular orbital (HOMO) and lowest unoccupied molecular orbital (LUMO) for compounds **1** and **2** (Fig. 7), were analyzed by Gaussian (Hehre et al., 1972). It is observable that HOMO has major contribution mainly localized on the ring B of compound **1**, while on ring A of compound **2** with little charge density on adjacent double bonds. The energy of HOMO is the ability of a compound to lose electron, and therefore considered equal to the ionization potential. While on the other hand, energy of LUMO describes the ability of a compound to gain electrons. Therefore, the negative of the energy of LUMO is taken as electron affinity. The figure shows that compounds **1** and **2** have LUMO contribution on C-1 and C-5, which represent that the double bonds are more susceptible to reduction so it can be reduced by the action of enzyme trypanothione reductase (Trypanothione is potential nucleophile in living cell of *Trpanosoma cruzi*). More ever the electron with drawing *para* nitro group on aromatic ring A or B makes the double bond more reactive for nucle-

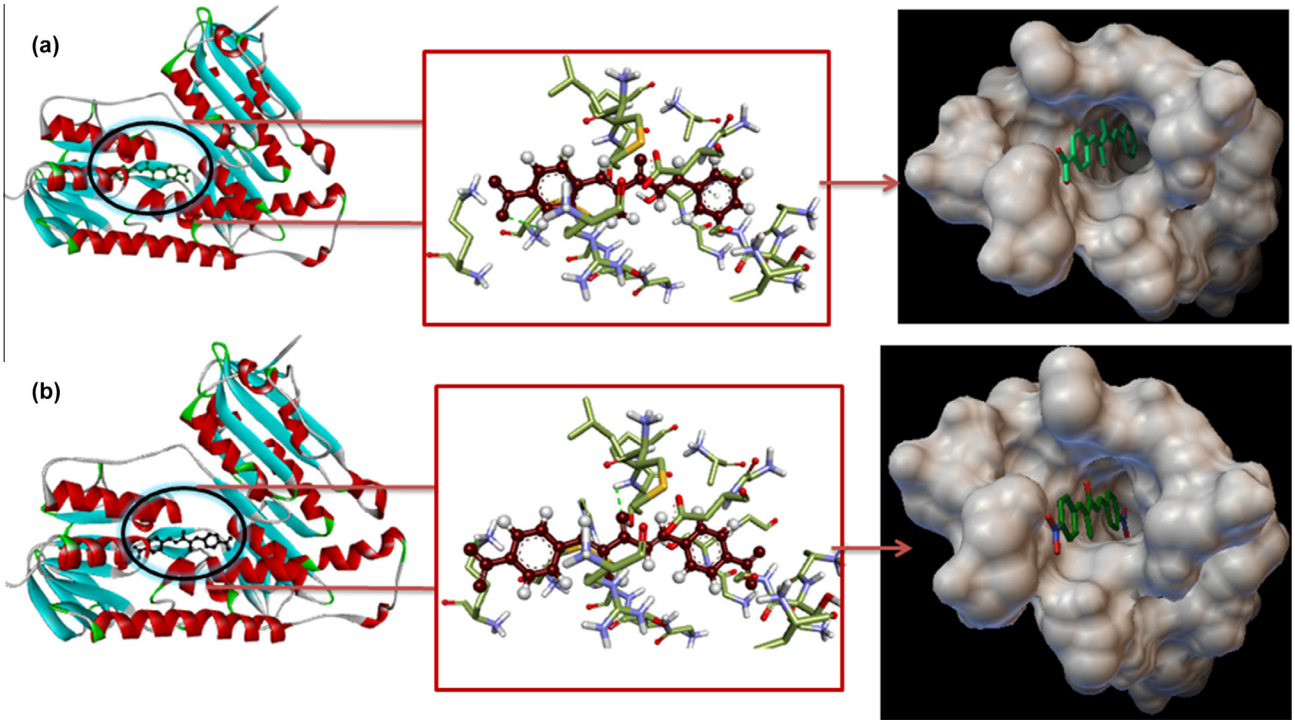


**Figure 5a** *In silico* analysis of the interaction of compounds **1** (above) and **2** (below) with active site of 1BZL.

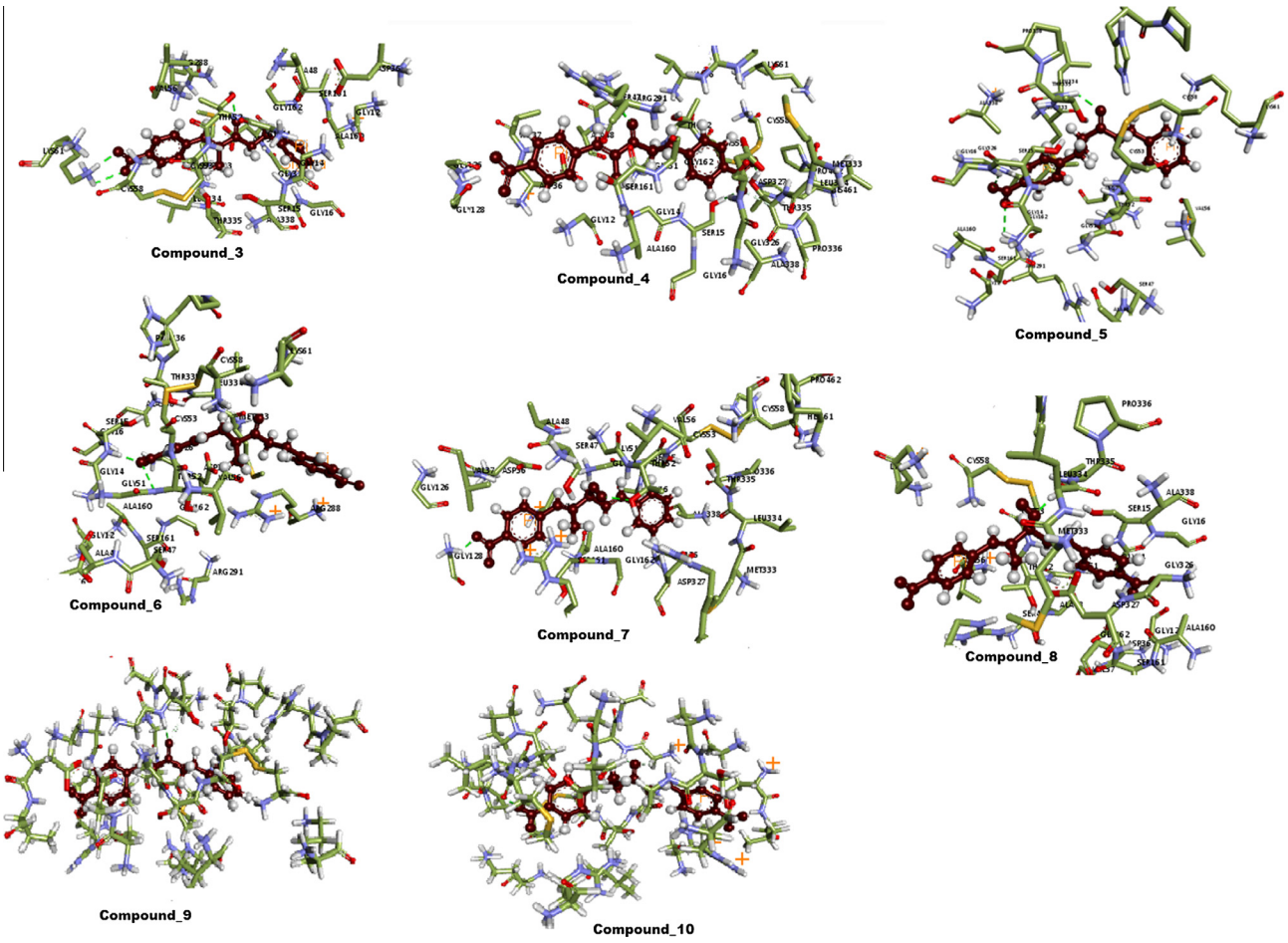


**Figure 5b** *In silico* analysis of the interaction of compounds **3–10** with active site of 1BZL.

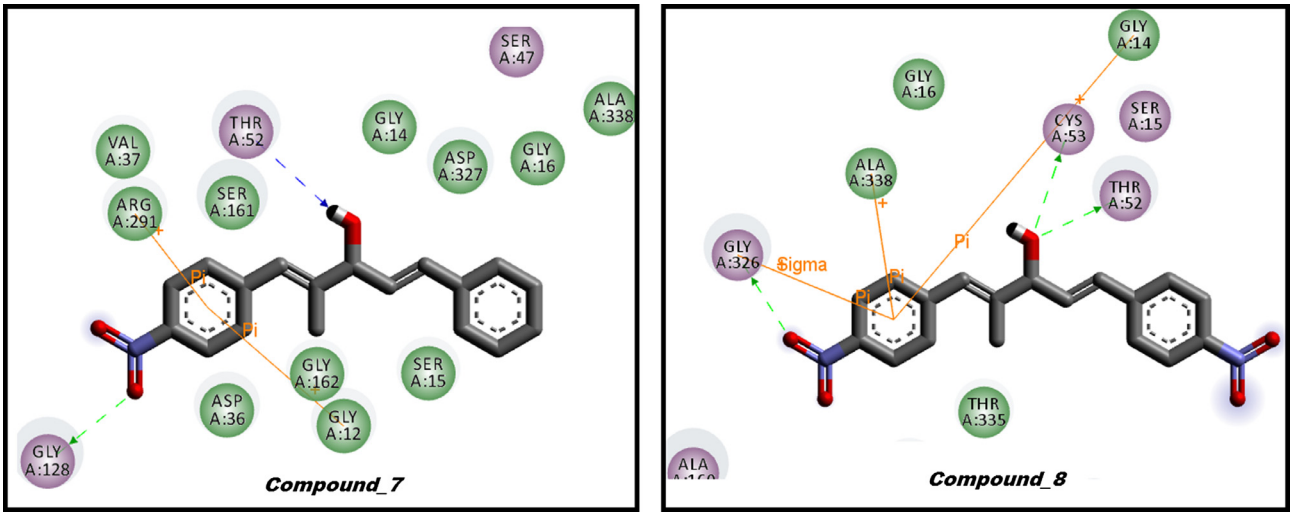


**Figure 6** Comparison of compounds **7** and **8** interaction in 2D.

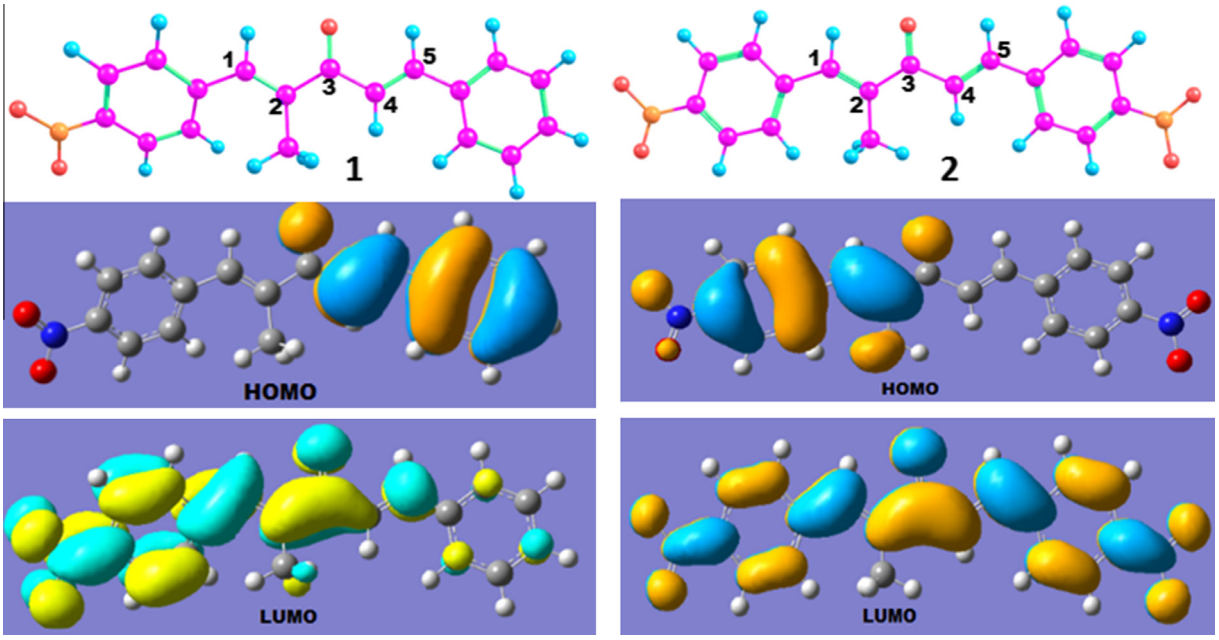


**Figure 7** Electronic distributions for compounds **1** and **2** [(1E,4E)-2-methyl-1,5-bis(4-nitrophenyl)penta-1,4-dien-3-one]. Semi-empirical calculations were performed using the Gaussian software package with the semi empirical B3LYP/6-31G(d,p) method and full geometric optimization.

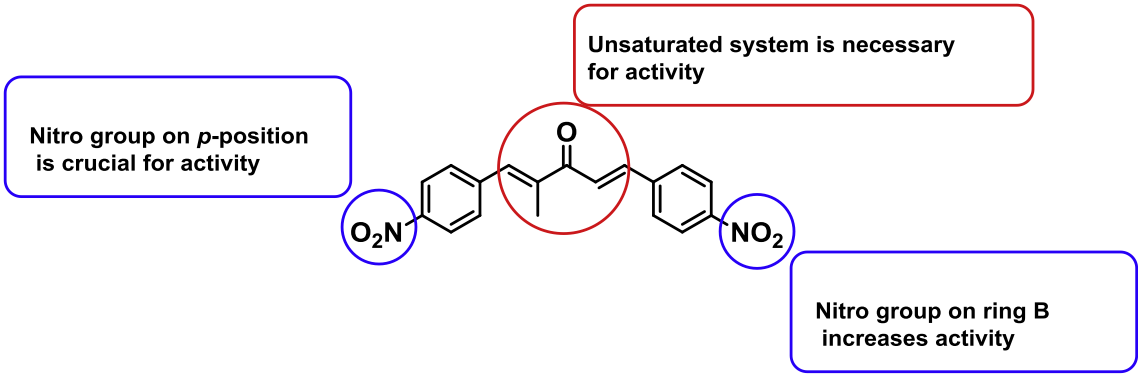


**Figure 8** Pro-drugs pharmacophoric moieties.

ophile attack. That's why when the nitro reduces the activity diminishes completely. The stability of all compounds was also calculated by Avogadro (Hanwell et al., 2012).

### 3. Conclusions

Metabolomic study of potent compounds **1** and **2** discloses interesting target by their mechanistic study. The action of parasite can modify the compounds in the result of metabolism. The metabolites obtain afford the reduction of both double bonds. Our previous study gives insight that the thiol level decreases once these compounds enter to parasite. When compounds **1** and **2** were reduced prior to treatment to *T. cruzi*, the decrease in potency was observed. So we can conclude that all the unsaturated moieties act as pharmacophores. We here propose that the covalent binding of compounds **1** and **2** with low molecular weight thiols as well as with protein thiols is a principal cause of the drug's toxicity against *T. cruzi*. Fig. 8 summarizes the necessary structural features for good activities of these diarylpenthadienones. More ever, to the best of our knowledge this is the first study showing the reduction of double bonds inside pathogen leading to potent parasitic activity and best structure–activity relationships in a new class of anti-parasitics.

### 4. Experimental

#### 4.1. General

All chemicals were purchased from Organics, Sigma–Aldrich, Acros Chemicals and Fisher Scientific Ltd and used without further purification. The deuterated solvents of Apolo were used for the NMR analysis. Thin layer chromatography was performed with precoated silica gel G-25-UV254 plates and detection was carried out at 254 nm under UV, and by vanillin in $H_2SO_4$ solution. $^1$H NMR, $^{13}$C NMR were performed on a Brüker AVANCE 400 operating at 400.15 MHz and

Please cite this article in press as: Din, Z.U. et al., The structure design of biotransformed unsymmetrical nitro-contained 1,5-diaryl-3-oxo-1, 4-pentadienyls for the anti-parasitic activities. Arabian Journal of Chemistry (2016), http://dx.doi.org/10.1016/j.arabjc.2016.03.005

100.62 MHz, respectively. $CDCl_3$ was used as solvent and tetramethylsilane (TMS) as internal reference. Compounds **1**, **2** and **3–10** were dissolved in organic solvents at about 5–10 mg $mL^{-1}$ each and shifted into a 5-mm NMR tube. Chemical shifts (δ in ppm) were measured with accuracy of 0.01 ($^1H$) and 0.1 ppm ($^{13}C$).

### 4.2. Chemistry

#### 4.2.1. Synthesis of (1E,4E)-2-methyl-1-(4-nitrophenyl)-5-phenylpenta-1,4-dien-3-one (1)

A Solution of A11K2 (200 mg, 0.976 mmol), and benzaldehyde (124 mg, 1.17 mmol) in ethanol (6 mL) was stirred for 5 min at room temperature, added sodium hydro oxide solution (2 mL, 1.25 mmol) and stirring was continued for six hours. The solvent was evaporated in vacuo. The residue dissolved in ethyl acetate, extracted with $NaHSO_3$ solution and dried with $Na_2SO_4$; solvent was evaporated in vacuo and the crude product was recrystallized from Ethyl acetate to give pure **1**.

Percent yield: 92%; $^1H$ NMR (400 MHz, $CDCl_3$) δ 8.28 (d, $J$ = 8 Hz, 2H, ArH), 7.73 (d, $J$ = 16 Hz, 2H, ArH), 7.62 (m, 2H, ArH), 7.58 (d, $J$ = 12 Hz, 2H, =CH), 7.55 (s, 1H, $CH_3C$=CH), 7.42 (m, 3H, ArH), 7.36 (d, $J$ = 16 Hz, 2H, =CH), 2.19 (d, $J$ = 4 Hz, 3H, =$CCH_3$); $^{13}C$ NMR (400 MHz, $CDCl_3$) δ 14 (1C, =CCH3); 121 (1C, =C); 125 (2C, ArC); 128 (2C, ArC); 129 (2C, ArC); 130 (2C, ArC); 131 (1C, ArC); 135 (1C, =C); 135 (1C, =C); 142 (1C, ArC); 143 (1C, =C); 145 (1C, ArC); 147 (1C, ArC); 192 (1C, CO); HRMS ESI(+): calcd 294.11247; found 294.11339; UV–Vis $\lambda_{max}$ (nm)[ε ($mol^{-1}$ $dm^3$ $cm^{-1}$)] in $CH_2Cl_2$: 308.

#### 4.2.2. Synthesis of (1E,4E)-2-methyl-1,5-bis(4-nitrophenyl) penta-1,4-dien-3-one (2)

Percent yield: 65%; $^1H$ NMR (400 MHz, $CDCl_3$) δ 8.31 (t, $J$ = 0 Hz, $J$ = 4 Hz, 1H, ArH), 8.29 (t, $J$ = 0 Hz, $J$ = 4 Hz, 2H, ArH), 8.23 (t, $J$ = 0 Hz, $J$ = 4 Hz, 1H, ArH), 7.74 (m, 3H, ArH and $CH_3$–C=CH), 7.60 (d, $J$ = 8 Hz, 3H, =CH and ArH), 7.49 (d, $J$ = 16 Hz, 1H, =CH), 2.21 (d, $J$ = 1.6 Hz, 3H, =$CCH_3$); $^{13}C$ NMR (400 MHz, $CDCl_3$) δ 191, 149, 147, 142, 141, 141, 141, 136, 130, 129, 125, 124, 124, 14; HRMS ESI(+): calcd 339.09955; found 339.09955. UV–Vis $\lambda_{max}$ (nm)[ε ($mol^{-1}$ $dm^3$ $cm^{-1}$)] in $CH_2Cl_2$: 304.

#### 4.2.3. (E)-2-methyl-1-(4-nitrophenyl)-5-phenylpent-1-en-3-one (3)

Percent yield: 69%; $^1H$ NMR (400 MHz, $CDCl_3$) δ 8.17 (d, $J$ = 8.8 Hz, 2H), 7.42 (d, $J$ = 8.5 Hz, 2H), 7.38 (s, 1H), 7.27–7.20 (m, 2H), 7.20–7.10 (m, 4H), 3.07 (t, $J$ = 7.8 Hz, 2H), 2.93 (d, $J$ = 7.3 Hz, 2H), 1.98 (d, $J$ = 1.4 Hz, 3H); $^{13}C$ NMR (400 MHz, $CDCl_3$) 201, 147, 143, 141, 140, 136, 130, 129, 129, 126, 124, 40, 31, 14.

#### 4.2.4. (E)-2-methyl-1,5-bis(4-nitrophenyl)pent-1-en-3-one (4)

Percent yield: 72%; $^1H$ NMR (400 MHz, $CDCl_3$) δ 8.26 (d, $J$ = 8.8 Hz, 2H), 8.16 (d, $J$ = 8.7 Hz, 2H), 7.52 (d, $J$ = 8.7 Hz, 2H), 7.50 (s, 1H), 7.41 (d, $J$ = 8.8 Hz, 2H), 3.19 (d, $J$ = 6.7 Hz, 2H), 3.14 (d, $J$ = 6.5 Hz, 2H), 2.06 (d, $J$ = 1.4 Hz, 3H). $^{13}C$ NMR (400 MHz, $CDCl_3$) δ 200, 149, 147, 147, 142, 140, 136, 130, 129, 124, 124, 39, 30, 13.

#### 4.2.5. 2-Methyl-1-(4-nitrophenyl)-5-phenylpentan-3-one (5)

Percent yield: 30%; $^1H$ NMR (400 MHz, $CDCl_3$) δ 8.09 (d, $J$ = 8.7 Hz, 2H), 7.25–7.14 (m, 5H), 7.10 (d, $J$ = 6.8 Hz, 2H), 3.06 (dd, $J$ = 13.4, 7.6 Hz, 1H), 2.88–2.73 (m, 4H), 2.69–2.52 (m, 2H), 1.08 (d, $J$ = 7.0 Hz, 3H). $^{13}C$ NMR (400 MHz, $CDCl_3$) δ 212, 148, 146, 149, 130, 128, 128, 126, 124, 48, 43, 38, 30, 17.

#### 4.2.6. 2-Methyl-1,5-bis(4-nitrophenyl)pentan-3-one (6)

Percent yield: 39%; $^1H$ NMR (400 MHz, $CDCl_3$) δ 8.10 (dd, $J$ = 8.8, 1.1 Hz, 4H), 7.29 (dd, $J$ = 8.8, 3.8 Hz, 4H), 3.09 (dd, $J$ = 13.5, 7.6 Hz, 1H), 3.00–2.81 (m, 4H), 2.71–2.57 (m, 2H), 1.11 (d, $J$ = 7.0 Hz, 3H). $^{13}C$ NMR (400 MHz, $CDCl_3$) δ 211, 149, 148, 147, 146, 130, 129, 124, 124, 48, 42, 38, 29, 17.

#### 4.2.7. (1E,4E)-2-methyl-1-(4-nitrophenyl)-5-phenylpenta-1, 4-dien-3-ol (7)

Percent yield: 72%; $^1H$ NMR (400 MHz, $CDCl_3$) δ 8.10 (d, $J$ = 8.9 Hz, 2H), 7.37–7.30 (m, 4H), 7.29–7.22 (m, 2H), 7.21–7.14 (m, 1H), 6.63 (d, $J$ = 15.1 Hz, 2H), 6.18 (dd, $J$ = 15.9, 6.7 Hz, 1H), 4.78 (d, $J$ = 6.7 Hz, 1H), 1.85 (d, $J$ = 1.3 Hz, 3H). $^{13}C$ NMR (400 MHz, $CDCl_3$) δ 146, 144, 143, 136, 132, 129, 129, 128, 128, 126, 124, 123.

#### 4.2.8. (1E,4E)-2-methyl-1,5-bis(4-nitrophenyl)penta-1,4-dien-3-ol (8)

Percent yield: 76%; $^1H$ NMR (400 MHz, $CDCl_3$) δ 8.22 (dd, $J$ = 8.8, 4.2 Hz, 4H), 7.57 (d, $J$ = 8.7 Hz, 2H), 7.47 (d, $J$ = 8.6 Hz, 2H), 6.84 (d, $J$ = 15.9 Hz, 1H), 6.76 (s, 1H), 6.47 (dd, $J$ = 15.9, 6.0 Hz, 1H), 4.97 (d, $J$ = 5.9 Hz, 1H), 1.97 (d, $J$ = 1.3 Hz, 3H). $^{13}C$ NMR (400 MHz, $CDCl_3$) δ 147, 146, 144, 143, 142, 134, 130, 130, 127, 125, 124, 124, 78, 15.

#### 4.2.9. 1-(4-Aminophenyl)-2-methyl-5-phenylpentan-3-one (9)

Percent yield: 90%; $^1H$ NMR (400 MHz, $CDCl_3$) δ 7.28–7.23 (m, 2H), 7.21–7.14 (m, 1H), 7.12 (dd, $J$ = 7.8, 0.9 Hz, 2H), 6.94 (d, $J$ = 8.4 Hz, 2H), 6.73 (d, $J$ = 8.4 Hz, 2H), 2.83 (ddd, $J$ = 10.9, 10.2, 4.7 Hz, 3H), 2.77–2.65 (m, 2H), 2.57 (ddd, $J$ = 17.2, 8.6, 6.4 Hz, 1H), 2.47 (dd, $J$ = 13.4, 7.2 Hz, 1H), 1.03 (d, $J$ = 6.9 Hz, 3H). $^{13}C$ NMR (400 MHz, $CDCl_3$) δ 214, 143, 141, 131, 130, 128, 128, 126, 116, 49, 44, 39, 30, 16.

#### 4.2.10. 1,5-Bis(4-aminophenyl)-2-methylpentan-3-one (10)

Percent yield: 92%; $^1H$ NMR (400 MHz, $CDCl_3$) δ 6.90 (dd, $J$ = 8.3, 7.1 Hz, 4H), 6.60 (dd, $J$ = 8.4, 1.8 Hz, 4H), 3.62 (s, 4H), 2.83 (dd, $J$ = 13.3, 7.1 Hz, 1H), 2.79–2.59 (m, 4H), 2.58–2.49 (m, 1H), 2.45 (dd, $J$ = 13.4, 7.2 Hz, 1H), 1.02 (d, $J$ = 6.8 Hz, 3H). $^{13}C$ NMR (400 MHz, $CDCl_3$) δ 214, 144, 144, 131, 131, 130, 129, 115, 115, 48, 44, 38, 29, 16.

### 4.3. Parasites and cells

*L. amazonensis* promastigote forms (MHOM/BR/Josefa) were maintained at 25 °C in Warren's medium (brain heart infusion plus haemin and folic acid) pH 7.0, supplemented with 10% Fetal Bovine Serum (FBS, Gibco Invitrogen, Grand Island, NY, USA). Epimastigote form of *T. cruzi* (Y strain) was maintained at 28 °C in liver infusion tryptose medium (LIT) supplemented with 10% inactivated FBS.

Please cite this article in press as: Din, Z.U. et al., The structure design of biotransformed unsymmetrical nitro-contained 1,5-diaryl-3-oxo-1, 4-pentadienyls for the anti-parasitic activities. Arabian Journal of Chemistry (2016), http://dx.doi.org/10.1016/j.arabjc.2016.03.005

### 4.4. Anti-proliferative assay

The effects of synthesized compounds were evaluated in promastigotes of *L. amazonensis* and epimastigotes of *T. cruzi*. The inoculum ($1 \times 10^6$ cells/mL) was introduced into 24-well plate containing the compounds dissolved in dimethylsulfoxide (DMSO) and Warren's medium or LIT in several concentrations (1.0–100.0 μM). The final concentration of DMSO did not exceed 1%. Cell grown was determined by counting the parasites with a Neubauer hemocytometer after incubation for 72 h at 25 °C for *L. amazonensis* or for 96 h at 28 °C for *T. cruzi*. The results were expressed as percentage of inhibition in relation to the control cultured. The $IC_{50}$ was determined by logarithm regression analysis of the data obtained. These procedures were repeated scaling-up the **1** and **2** dosage to reach $IC_{90}$ and the medium was lyophilized and further extracted for metabolomic study.

### 4.5. Cytotoxicity assay

The cytotoxicity was evaluated in VERO cells. For VERO cells, a suspension of $2.5 \times 10^5$ cells/mL was cultured in DMEM. After 24 h, the different compounds were added to each well (10.0–1000.0 μM) and the plates were incubated for 72 h for VERO cells in a 5% $CO_2$–air mixture at 37 °C. Following incubation, MTT assay was performed (2 mg/mL stock solution, 50 μL/well). After 4 h of incubation, the MTT processing was stopped, and the formazan crystals were solubilized by adding DMSO (150 μL/well). The relative amount of formazan/well produced by viable cells was determined spectrophotometrically at 570 nm by blanking against an appropriate control. The $CC_{50}$ values (50% cytotoxic concentration) were estimated and the selectivity index (SI) was used to compare cytotoxicity between cells and protozoa (ratio: $CC_{50}$ of cells divided by $CC_{50}$ of the compound in the protozoa).

### 4.6. Docking studies

In order to evaluate the described biological results, compounds **1–10** were evaluated for docking studies against enzyme trypanothione reductase, which is reported under pdb code 1BZL. Auto Dock Tool 4.2 from scripts research institute was used for docking analysis (Morris et al., 2009). Docking was used to predict both ligand and binding affinity orientation of ligand to the receptor, to form complex in three dimensional spaces. Autodock with the inhibition score, which uses bond strengths, was used for the docking calculations. Calculation was performed by removing water molecules first and adding polar hydrogen atoms using the option available in autodock tool. Gasteiger charges were also assigned for ligands and then the protein ligand was processed for obtaining file .pdbqt, which are input files for autodock 4.2. Enzyme 1BZL was optimized by considering only chain A and active site occupied by inhibitors. The protein binding sites were defined using those occupied by the co-crystallized ligand for 1BZL. The program Accelrys Discovery Studio® v4.1 (Dassault Systèmes BIOVIA, 2015) was used to analyze the docking results and poses (orientations/conformations) and interactions.

### 4.7. Computational study

Calculations were performed using the Gaussian 03 package (Frisch et al., 2004). Geometries of all the species investigated were optimized without any symmetry constraints, and the resulting structures were further assessed using vibrational frequency analysis to probe whether or not the structures represent true minimum-energy geometries. If any imaginary frequency was found, further optimizations were performed along those normal coordinates (without symmetry constraints). All the calculations were done using two hybrid DFT functionals: B3LYP (Parr and Yang, 1989) and B3PW91 (Parr and Yang, 1989). The approaches are subsequently referred to as B3LYP/6-31G*. For all the structures under investigation, the singlet states were considered for calculation. Molecular structures and frontier orbital's were visualized using Gauss view software.

## Acknowledgments

The authors are grateful to Fundação de Amparo à Pesquisa do Estado de São Paulo (FAPESP, Proc. Num. 2010/11384-6), Conselho Nacional de Desenvolvimento Científico e Tecnológico (CNPq), and Coordenação de Aperfeiçoamento de Pessoal de Ensino Superior (CAPES) for financial support and Third World Academy of Science (TWAS) for Ph.D fellowship. The computational resources of the Centro Nacional de Processamento de Alto Desempenho em São Paulo are highly appreciated.

## Appendix A. Supplementary material

Supplementary data associated with this article can be found, in the online version, at http://dx.doi.org/10.1016/j.arabjc.2016.03.005.

## References

Aponte, J.C., Verástegui, M., Málaga, E., Zimic, M., Quiliano, M., Vaisberg, A.J., Gilma, R.H., Hammond, G.B., 2008. Synthesis, cytotoxicity, and anti-*Trypanosoma cruzi* activity of new chalcones. J. Med. Chem. 51, 6230–6234.

Bidóia, D.L., Desoti, V.C., Martins, S.C., Ribeiro, M.F., Zia, U., Edsom, R.-F., Nakamura, T.U., Nakamura, C.V., Silvaa, S.O., 2015. Dibenzylideneacetones are potent trypanocidal compounds that affect the *Trypanosoma cruzi* redox system. Antimicrob. Agents Chemother. 11. http://dx.doi.org/10.1128/AAC.01360-15.

Boechat, N., Carvalho, A.S., Salomão, K., de Castro, S.L., Araujo-Lima, C.F., Mello, F.V.C., Felzenszwalb, I., Aiub, C.A.F., Conde, T.R., Zamith, H.P.S., Skupin, R., Haufe, G., 2015. Studies of genotoxicity and mutagenicity of nitroimidazoles: demystifying this critical relationship with the nitro group. Memórias do Instituto Oswaldo Cruz 110, 492–499. http://dx.doi.org/10.1590/0074-02760140248.

Campos, M.C.O., Leon, L.L., Taylor, M.C., Kelly, J.M., 2014. Benznidazole-resistance in *Trypanosoma cruzi*: evidence that distinct mechanisms can act in concert. Mol. Biochem. Parasitol. 193, 17–19. http://dx.doi.org/10.1016/j.molbiopara.2014.01.002.

Dassault Systèmes BIOVIA, 2015. Discovery Studio Modeling Environment, Release 4.1.

Frisch, M.J., Trucks, G.W., Schlegel, H.B., Scuseria, G.E., Robb, M. A., Cheeseman, J.R., Montgomery Jr., J.A., Vreven, T., Kudin, K. N., Burant, J., 2004. GAUSSIAN 03, Revision D.01.

Garcia, S., Ramos, C.O., Senra, J.F.V., Vilas-Boas, F., Rodrigues, M. M., Campos-de-Carvalho, A.C., Ribeiro-Dos-Santos, R., Soares, M.B.P., 2005. Treatment with benznidazole during the chronic phase of experimental Chagas' disease decreases cardiac alterations. Antimicrob. Agents Chemother. 49, 1521–1528. http://dx.doi.org/10.1128/AAC.49.4.1521-1528.2005.

Hall, B.S., Bot, C., Wilkinson, S.R., 2011. Nifurtimox activation by trypanosomal type I nitroreductases generates cytotoxic nitrile metabolites. J. Biol. Chem. 286, 13088–13095. http://dx.doi.org/10.1074/jbc.M111.230847.

Hall, B.S., Meredith, E.L., Wilkinson, S.R., 2012. Targeting the substrate preference of a type I nitroreductase to develop antitrypanosomal quinone-based prodrugs. Antimicrob. Agents Chemother. 56, 5821–5830. http://dx.doi.org/10.1128/AAC.01227-12.

Hanwell, M.D., Curtis, D.E., Lonie, D.C., Vandermeerschd, T., Zurek, E., Hutchison, G.R., 2012. Avogadro: an advanced semantic chemical editor, visualization, and analysis platform. J. Cheminform. 4, 1–17. http://dx.doi.org/10.1186/1758-2946-4-17.

Hehre, W.J., Ditchfield, R., Pople, J.A., 1972. Self—consistent molecular orbital methods. XII. Further extensions of gaussian—type basis sets for use in molecular orbital studies of organic molecules. J. Chem. Phys. 56, 2257–2261. http://dx.doi.org/10.1063/1.1677527.

Marin-Neto, J.A., Rassi Jr., A., Avezum Jr., A., Mattos, A.C., Rassi, A., 2009. The BENEFIT trial: testing the hypothesis that trypanocidal therapy is beneficial for patients with chronic Chagas heart disease. Memórias do Instituto Oswaldo Cruz 104, 319–324. http://dx.doi.org/10.1590/S0074-02762009000900042.

Martin, N.J.A., List, B., 2006. Highly enantioselective transfer hydrogenation of alpha, beta-unsaturated ketones. J. Am. Chem. Soc. 128, 13368–13369. http://dx.doi.org/10.1021/ja065708d.

McGreevy, P.B., Marsden, P.D., 1986. Chemotherapy of Parasitic Diseases. Springer, US.

Mejia, A.M., Hall, B.S., Taylor, M.C., Gómez-Palacio, A., Wilkinson, S.R., Triana-Chávez, O., Kelly, J.M., 2012. Benznidazole-resistance in *Trypanosoma cruzi* is a readily acquired trait that can arise independently in a single population. J. Infect. Dis. 206, 220–228. http://dx.doi.org/10.1093/infdis/jis331.

Morris, G.M., Huey, R., Lindstrom, W., Sanner, M.F., Belew, R.K., Goodsell, D.S., Olson, A.J., 2009. AutoDock4 and AutoDockTools4: automated docking with selective receptor flexibility. J. Comput. Chem. 30, 2785–2791. http://dx.doi.org/10.1002/jcc.21256.

Murakami, M.T., Rodrigues, N.C., Gava, L.M., Honorato, R.V., Canduri, F., Barbosa, L.R.S., Oliva, G., Borges, J.C., 2013. Structural studies of the *Trypanosoma cruzi* Old Yellow Enzyme: insights into enzyme dynamics and specificity. Biophys. Chem. 184, 44–53. http://dx.doi.org/10.1016/j.bpc.2013.08.004.

N°340, F. Sheet, 2014. World Health Organization. WHO, March.

Parr, R.G., Yang, W., 1989. Density-Functional Theory of Atoms and Molecules. Oxford University Press.

Patterson, S., Wyllie, S., 2014. Nitro drugs for the treatment of trypanosomatid diseases: past, present, and future prospects. Trends Parasit. 30, 289–298. http://dx.doi.org/10.1016/j.pt.2014.04.003.

Priotto, G., Kasparian, S., Mutombo, W., Ngouama, D., Ghorashian, S., Arnold, U., Ghabri, S., Baudin, E., Buard, V., Kazadi-Kyanza, S., Ilunga, M., Mutangala, W., Pohlig, G., Schmid, C., Karunakara, U., Torreele, E., Kande, V., 2009. Nifurtimox–eflornithine combination therapy for second-stage African *Trypanosoma brucei* gambiense trypanosomiasis: a multicentre, randomised, phase III, non-inferiority trial. Lancet 374, 56–64. http://dx.doi.org/10.1016/S0140-6736(09)61117-X.

Romão, P.R.T., Tovar, J., Fonseca, S.G., Moraes, R.H., Cruz, A.K., Hothersall, J.S., Noronha-Dutra, A.A., Ferreira, S.H., Cunha, F. Q., 2006. Glutathione and the redox control system trypanothione/trypanothione reductase are involved in the protection of *Leishmania* spp. against nitrosothiol-induced cytotoxicity. Braz. J. Med. Biol. Res. 39, 355–363. http://dx.doi.org/10.1590/S0100-879X2006000300006.

Roussaki, M., Hall, B., Lima, S.C., da Silva, A.C., Wilkinson, S., Detsi, A., 2013. Synthesis and anti-parasitic activity of a novel quinolinone–chalcone series. Bioorg. Med. Chem. Lett. 23, 6436–6441. http://dx.doi.org/10.1016/j.bmcl.2013.09.047.

Singh, R., Manjunatha, U., Boshoff, H.I.M., Ha, Y.H., Niyomrattanakit, P., Ledwidge, R., Dowd, C.S., Lee, I.Y., Zhang, L., Kang, S., Keller, T.H., Jiricek, J., Barry, C.E., 2009. PA-824 kills nonreplicating *Mycobacterium tuberculosis* by intracellular NO release. Science 322, 1392–1395. http://dx.doi.org/10.1126/science.1164571.PA-824.

Torreele, E., Bourdin Trunz, B., Tweats, D., Kaiser, M., Brun, R., Mazué, G., Bray, M.a., Pécoul, B., 2010. Fexinidazole – a new oral nitroimidazole drug candidate entering clinical development for the treatment of sleeping sickness. PLoS Neglected Trop. Dis. 4, e923. http://dx.doi.org/10.1371/journal.pntd.0000923.

Warda, D.E., Rheea, C.K., 1989. Chemoselective reductions with sodium borohydride. Can. J. Chem. 67, 1206–1211.

Wilkinson, S.R., Taylor, M.C., Horn, D., Kelly, J.M., Cheeseman, I., 2008. A mechanism for cross-resistance to nifurtimox and benznidazole in trypanosomes. Proc. Natl. Acad. Sci. USA 105, 5022–5027. http://dx.doi.org/10.1073/pnas.0711014105.

Wyllie, S., Patterson, S., Fairlamb, A.H., 2013. Assessing the essentiality of *Leishmania donovani* nitroreductase and its role in nitro drug activation. Antimicrob. Agents Chemother. 57, 901–906. http://dx.doi.org/10.1128/AAC.01788-12.

Yamaguchi, K., Okamoto, N., Tokuoka, K., Sugiyama, S., Uchiyama, N., Matsumura, H., Inaka, K., Urade, Y., Inoue, T., 2011. Structure of the inhibitor complex of old yellow enzyme from *Trypanosoma cruzi*. J. Synchrotron Radiat. 18, 66–69. http://dx.doi.org/10.1107/S0909049510033595.

Zia, U.D., Fill, T.P., de Assis, F.F., Lazarin, D.B., Kaplum, V., Garcia, F., Nakamura, C.V., Oliveira, K.T., Filho, E.R., 2014. Unsymmetrical 1,5-diaryl-3-oxo-1,4-pentadienyls and their evaluation as antiparasitic agents. Bioorg. Med. Chem. 22, 1121–1127. http://dx.doi.org/10.1016/j.bmc.2013.12.020.

Please cite this article in press as: Din, Z.U. et al., The structure design of biotransformed unsymmetrical nitro-contained 1,5-diaryl-3-oxo-1, 4-pentadienyls for the anti-parasitic activities. Arabian Journal of Chemistry (2016), http://dx.doi.org/10.1016/j.arabjc.2016.03.005